

# 1 Isotherm studies of arsenic adsorption on 2 natural adsorbents: laterite, sandstone, and 3 shale

4

11

12

13 Research Article

14

15

## 16 ABSTRACT

Arsenic contamination of drinking water has been an increasing concern worldwide because of toxicity. In Côte d'Ivoire, high concentrations of arsenic are increasingly being found in the water around mining operations. Identifying and determining the modes of arsenic retention on geological matrices is essential for designing adsorption systems. In this study, the adsorption process of an aqueous arsenic solution on laterite, sandstone, and shale was examined. Under optimized conditions of pH, contact time, initial arsenic concentration, and temperature, batch adsorption isotherms were performed. Thermodynamic parameters such as  $\Delta H^\circ$ ,  $\Delta S^\circ$ , and  $\Delta G^\circ$  were calculated. The Langmuir, Freundlich, Temkin, Elovich, and Dubinin–Radushkevich (D–R) models were explored. Isotherms are classified as type L. The Langmuir isotherm was highly favorable at all temperatures with maximum monolayer capacities of 1.627 for laterite, 0.539 for sandstone, and 0.135 for shale. The correlation coefficient  $R^2$  was closest to 1. Temkin's binding energy values (22.101–67.977 KJ/mol) chemisorption is suggested, while Dubinin-Radushkevich energies below 8 KJ/mol point to physical adsorption. Both types of adsorption appear to be involved. This study recommends the applicability of laterite first, followed by sandstone and shale, for removing arsenite ions from water.

17  
18 *Keywords: Adsorption, adsorption isotherm, arsenic, laterite, shale, sandstone*

## 21 1. INTRODUCTION

22 Arsenic contamination in drinking water is a global concern, reported in countries like India, China, Taiwan, Vietnam, Chile,  
23 Argentina, Canada, Ghana, Burkina Faso, and Côte d'Ivoire. Its presence results from sedimentary and altered volcanic  
24 rocks, and geothermal waters, as well as human activities like mining, metallurgy, chemical production, and pesticide use  
25 [1] [2] [3]. Given the various harmful impacts that the presence of arsenic in water could have on human health, it is important  
26 to find less expensive treatment methods. Among existing treatment methods, adsorption stands out in developing countries  
27 due to its affordability, simplicity, and environmental friendliness [4]. To understand the mechanism, equilibrium data known  
28 as adsorption isotherms are essential. These describe interactions between arsenic ions and adsorbent surfaces and help  
29 develop remediation techniques [5] [6]. Thus, different models were tested in order to find a mathematical relationship  
30 between the concentration of the solute in the solution at equilibrium and the amount of solute adsorbed at equilibrium. The  
31 interest of using different models is crucial to obtain information concerning the maximum adsorption capacity ( $q_m$ ), the  
32 possible interactions between the adsorbates, the adsorption energy, as well as the adsorption mechanisms and reactions  
33 involved at the liquid-solid interface [7]. Various natural geosorbents like kaolinite, illite, muscovite, montmorillonite, clay,  
34 laterite, sandstone, and shale have shown promise. The physical and mineralogical characterisation of laterite, sandstone,

and shale was carried out by Coulibaly et al. [8] [9] making it possible to understand the variations in performance of the three adsorbents. According to previous studies, the supports have high iron, aluminium and calcium contents and are effective for arsenic removal. These rocks are not very resistant to crushing and are available in sufficient quantities and at low cost in Côte d'Ivoire. However, studies on isotherms involving sandstone and shale remain limited. This study examines the adsorption isotherm of arsenic from water by geomaterials (laterite, sandstone, and shale) given its importance for the development of water treatment systems. The main objectives were to (i) determine the arsenic adsorption isotherms with the laterite, sandstone, and shale, (ii) assess the models that are appropriate.

## 2. MATERIAL AND METHODS

### 2.1 Effect of temperature

In adsorption processes, temperature is a key variable for identifying the nature of the adsorption mechanism. When the mass of the adsorbent, the initial concentration, and the pH are kept constant, the rate of metal ion adsorption is governed by whether the reaction is endothermic or exothermic. If the process is endothermic, increasing the temperature improves the adsorption yield. Conversely, if the process is exothermic, a rise in temperature leads to a decrease in adsorption efficiency. Thermodynamic quantities, standard Gibbs free energy ( $\Delta G^\circ$ ), standard entropy ( $\Delta S^\circ$ ), and standard enthalpy ( $\Delta H^\circ$ ), were determined for the adsorption of arsenic ions on various adsorbents at the studied temperatures [10].

### 2.2 Energetic Aspect of Adsorption

Any variation or transformation within a system is generally associated with a change in free energy. For an adsorption reaction involving molecules on a surface, the change in Gibbs free energy can be expressed by the following equation (1):

$$\Delta G = \Delta H - T\Delta S \quad (1)$$

Where:

$\Delta G$  is the Gibbs adsorption energy, made up of two key components: an entropic term ( $\Delta S$ ) that reflects changes and molecular rearrangements in the liquid phase and on the adsorbent surface, an enthalpic term ( $\Delta H$ ) that represents the interaction energies between the adsorbed molecules and the adsorbing surface.  $\Delta G$  ( $\text{KJ}\cdot\text{mol}^{-1}$ ) corresponds to the energy variation at constant pressure and determines the feasibility of the reaction. A thermodynamic system always tends to evolve spontaneously toward a lower energy state. Thus, for a reaction to occur spontaneously,  $G$  must be negative [10].

The thermodynamic relationship (1) combined with the Van't Hoff equation yields ( $\Delta G = -RT \ln K_d$ ) gives equation (2) :

$$\ln K_d = \frac{\Delta S}{R_g} - \frac{\Delta H}{R_g} * \frac{1}{T} \quad (2)$$

Where :

$K_d$  : is the sorption distribution constant ;

$R_g$  : is the ideal gas constant (8.314 J/mol·K);

$T$  : is the temperature (K).

Generally, adsorption is accompanied by a thermal process, which can be endothermic ( $\Delta H > 0$ ), favored at higher temperatures and exothermic ( $\Delta H < 0$ ), where higher temperatures reduce adsorption performance. The value of adsorption enthalpy  $\Delta H$  is crucial for distinguishing between physisorption, typically characterized by free energy values ranging from 5 to 40 kJ/mol and chemisorption, with energy values ranging from 40 to 120 kJ/mol [11].

### 2.3 Collection and preparation of supports

The laterite samples were taken at Sinematialy (9° 35' N and 5° 23' O) in the north of Côte d'Ivoire. The shale was collected in the Toumodi region in central Côte d'Ivoire (6° 39' 15" N and 4° 58' 33" O) at the Lomo nord site and the sandstone in southern Côte d'Ivoire, in the Akouedo locality (5° 21' 07" N and 3° 56' 30" O). The materials were crushed separately, washed and then dried for 24 h and reduced using a Retsch RS 100 crusher. The crushed material was sieved using Saulas sieves (NF.X 11.501). Fractions with a particle size of less than 250  $\mu\text{m}$  were selected for batch testing. The sieving process reduced the coarse particles and therefore the impurities.

### 2.4 Adsorption Isotherms

Batch adsorption experiments were conducted at three different temperatures: 20 °C, 30 °C, and 40 °C. As (III) stock solution (1000mg/L) was prepared by dissolving reagent grade As(III) oxid of 99.5% purified into deionized water. The volume of the solution was made up to 1L in a standard flask. The working solution containing arsenic were prepared by dissolving appropriate amount of arsenic from stock solutions in well water [12]. For each temperature, the initial concentration of arsenic (III) in water was varied from 1 to 54.7 mg/L. A fixed volume of 40 mL was used, and each solution was mixed with the optimal mass of adsorbent materials, laterite: 2 g, sandstone 3 g, and shale: 5.8 g [12].

After 24 hours of agitation, the filtrates were analyzed, and the amount of arsenic adsorbed was calculated using the following equation :

$$q_e = \frac{(C_0 - C_e) * V}{m} \quad (3)$$

Where:

- $q_e$  : adsorption capacity at equilibrium (mg/g) ;
- $C_e$  : arsenic concentration at equilibrium (mg/L) ;
- $C_0$  : initial arsenic concentration (mg/L) ;
- $m$  : mass of adsorbent (g) ;
- $V$  : volume of solution (L).

As (III) concentration of the filtered solutions was analysed with Optical Emission Spectrometer OPTIMA 2100 Dual View (ICP-OES 2100 DV). The adsorption equilibrium isotherm represents the amount of molecules adsorbed per unit mass of adsorbent as a function of the concentration of molecules in the liquid phase when the system is at equilibrium. The shape of the curve provides valuable information about the mechanisms involved. There are several ways to categorize adsorption equilibrium isotherms. Giles et al. [13] identified four types for adsorption of molecules in liquid phase (Fig. 1) :

- ✓ Type L isotherm: Characteristic of microporous adsorbents; reflects a strong affinity between the adsorbate and the adsorbent
- ✓ Type S isotherm: Corresponds to solids with heterogeneous porosity; suggests competitive adsorption involving interactions between adsorbate-adsorbate and adsorbate-adsorbent.
- ✓ Type H isotherm: An extreme case of the Type L isotherm; indicates a very high affinity between the adsorbate and the adsorbent
- ✓ Type C isotherm (or linear isotherm): Represents a linear distribution of solute between the solid phase and the liquid phase.

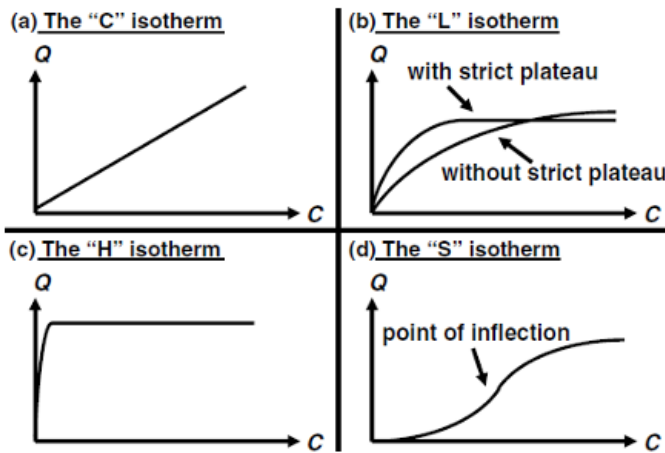


Fig. 1. Main different shapes of adsorption isotherms according to Wang and Guo [7].

## 2.5 Modeling of Adsorption Isotherms

The capacity of adsorbents to capture the different components of a mixture is the most decisive factor in the performance of most adsorption processes. To design and scale up adsorption systems, it's essential to understand the equilibrium properties between the adsorbate and the adsorbent. Adsorption isotherms, determined at a given temperature, generally characterize the amounts adsorbed at equilibrium [14]. The Langmuir, Freundlich, Temkin, Elovich, and Dubinin–Radushkevich (D–R) adsorption models were used.

The linear form of the Freundlich model is :  $\ln q_e = \ln K_f + (1/n) \ln C_e$ .

The slopes and intercepts of these lines make it possible to calculate the Freundlich parameters ( $K_f$  and  $n_f$ ).

The linear form of the Langmuir model is  $1/q_e = 1/q_{max} + 1/k_L q_{max} C_e$

where  $K_L$  is the Langmuir binding constant,  $C_e$  is the residual concentration in solution at adsorption equilibrium (mg/L),  $q_e$  is the amount of adsorbate at equilibrium (mg/g), and  $q_{max}$  is the maximum amount adsorbed (mg/g).

130 The Elovich isotherm assumes that the adsorption sites increase exponentially with adsorption, implying multilayer  
131 adsorption (Author). Its linear form is  $\ln q_e/q_m = \ln K_e(q_m - q_e/q_m)$ , where  $q$ (mg/g) and  $K_e$  (L/mg) represent the adsorption  
132 capacity and the equilibrium constant [15].  
133

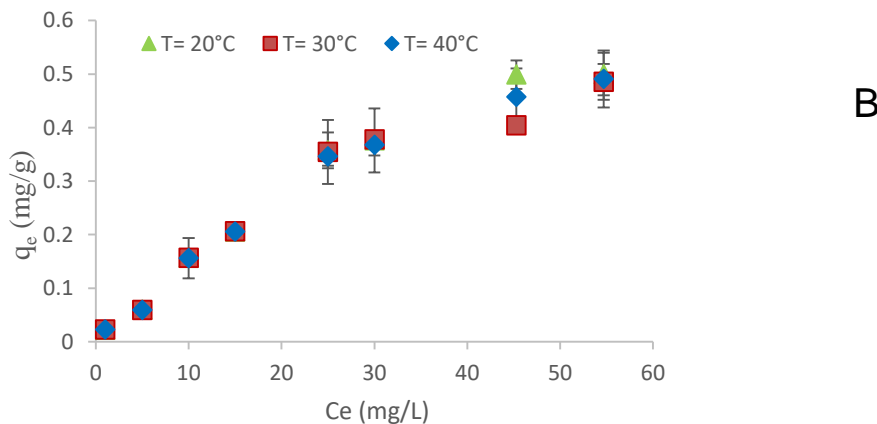
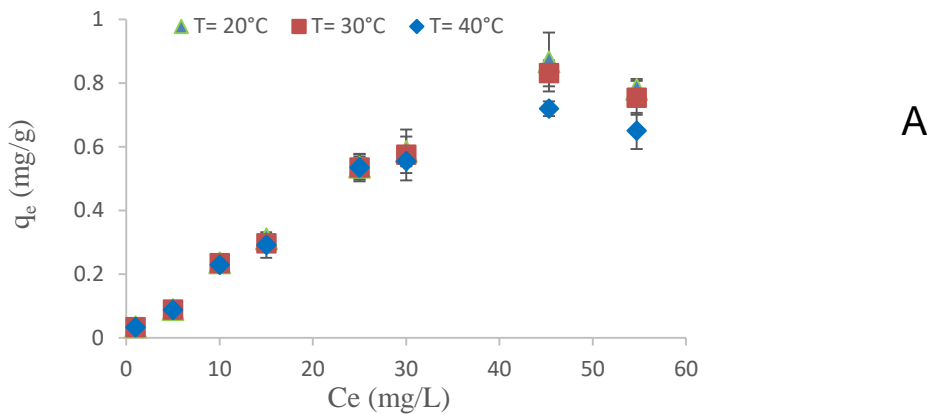
134 The Temkin model assumes that the free energy of sorption is a function of surface coverage [16]. The linear form is  $q_e =$   
135  $RT/b_T \ln K_T + RT/b_T \ln C_e$  where  $b_T$  is a constant associated with the adsorption heat, and  $K_T$  (L/mg) is the Temkin constant.  
136

137 The Dubinin-Radushkevich (D-R) model does not assume a homogeneous surface or constant adsorption potential. Its  
138 linear form is  $\ln q = \ln q_m - \beta \times \epsilon^2$  where  $\beta$  is the coefficient related to adsorption energy (mol<sup>2</sup>/J<sup>2</sup>),  $q_m$  is the theoretical  
139 saturation capacity (mg/g), and  $\epsilon$  is the Polanyi potential, related to the equilibrium concentration.  
140

### 141 3. RESULTS AND DISCUSSION

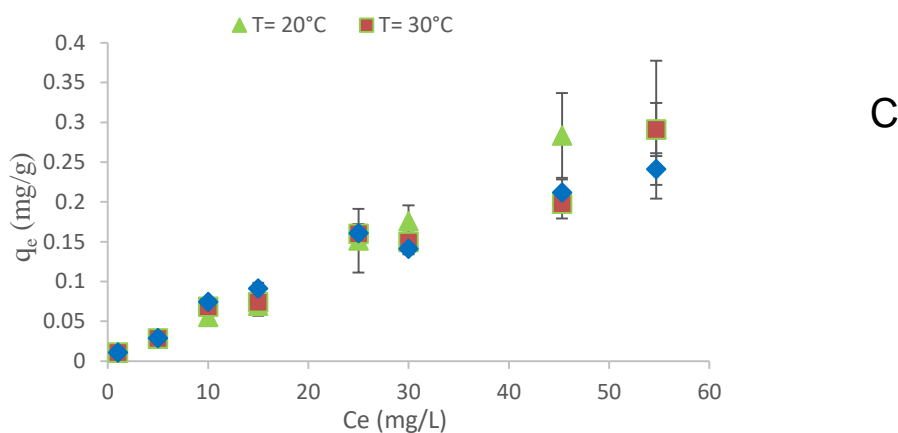
#### 142 3.1 Adsorption Isotherms

143 The adsorption isotherms obtained by varying the initial concentration of As at different temperatures are shown in Fig. 2.  
144 These isotherms are classified as type L, which typically indicates microporous adsorbents with strong adsorbate adsorbent  
145 affinity as reported by Coulibaly et al. [9], with a progressive saturation of adsorption sites. The curves show that arsenic  
146 adsorption isotherms on laterite, sandstone and shale have two phases. There is an initial phase between 0 and 30 mg/L,  
147 corresponding to a gradual increase in adsorption capacity in parallel with the concentration until a maximum is reached.  
148 This is followed by a second phase marked by a plateau corresponding to a state of equilibrium. Two (2) different behaviours  
149 emerge depending on the adsorbent above 30 mg/L. On laterite, the arsenic adsorption capacity decreases as the  
150 temperature rises. For a starting concentration of 45 mg/L, the quantity of arsenic adsorbed ( $q_e$ ) decreases from 0.867 to  
151 0.831 and then to 0.719 mg/g of material for temperatures of 20, 30 and 40°C respectively. For sandstone (B) and shale  
152 (C), no clear trend is observed at this concentration range. This decline may result from reduced stability of the bonds  
153 between active sites and arsenic as temperature rises. According to Belaid and Kacha [17], this phenomenon aligns with  
154 the Arrhenius law, suggesting that the surface reaction is exothermic, and thus, higher temperatures hinder its progress. In  
155 this case, physisorption would be the dominant mechanism. Similar observations were made by Mondal et al. [18] and Ziati  
156 et al. [19].  
157  
158  
159



160  
161

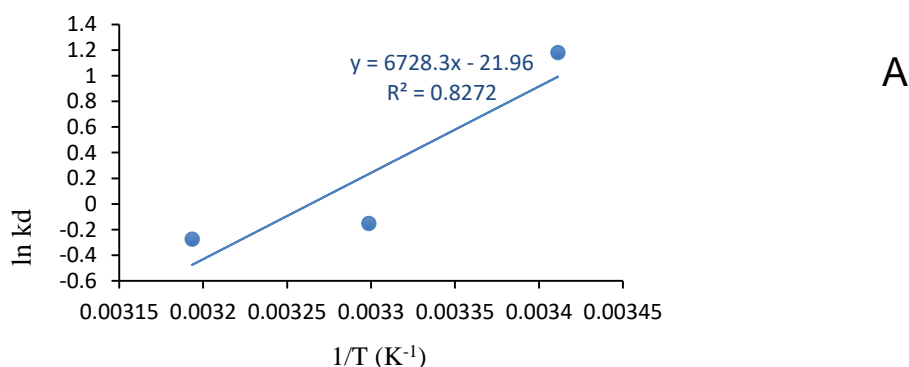
162  
163

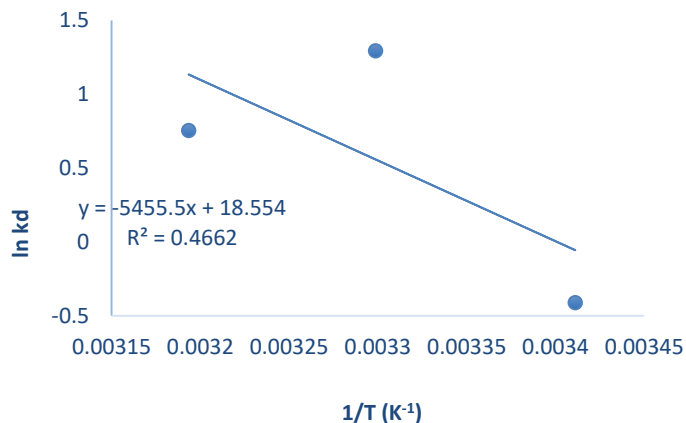


165  
166  
167  
168 **Fig. 2.** Adsorption isotherms of arsenic at different temperatures (20, 30, 40°C) on laterite (A), sandstone (B), and shale  
169 (C).

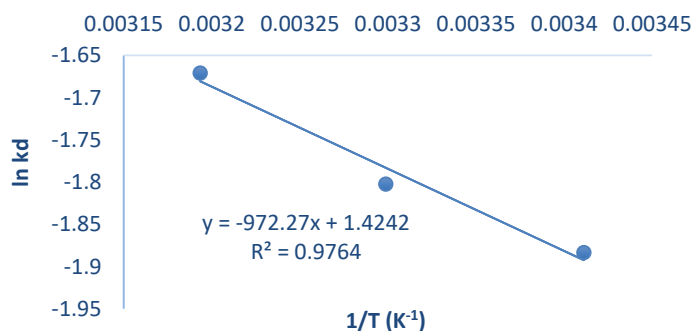
### 170 3.2 Thermodynamic Study of Arsenic Adsorption in Aqueous Solution

171  
172  
173 The plot of the natural logarithm of the sorption distribution constant ( $\ln K_d$ ) against  $1/\text{Temperature}$ , shown in Fig. 3, enables  
174 determination of the enthalpy ( $\Delta H^\circ$ ) (slope of the line) and the entropy ( $\Delta S^\circ$ ) (y-intercept). The resulting values are presented  
175 in Table I. The negative value ( $-8.083 \text{ kJ/mol}$ ) of  $\Delta H^\circ$  in the case of shale indicates an exothermic process. In contrast, the  
176 values obtained for laterite and sandstone, ranging between  $45.357$  and  $55.94 \text{ kJ/mol}$ , indicate the endothermic nature of  
177 arsenic sorption and suggest a chemisorption mechanism [20]. Unuabonah et al. [21] and Boparai et al. [22] noted by  
178 physical adsorption energies are below  $40 \text{ kJ/mol}$ , whereas chemical adsorption energies range from  $40$  to  $800 \text{ kJ/mol}$ . The  
179 value of  $\Delta S^\circ$  is negative for laterite ( $-0.180 \text{ kJ/mol}$ ) and sandstone ( $-0.154 \text{ kJ/mol}$ ). The negative entropy values ( $\Delta S$ )  
180 indicate a decrease in the degree of freedom of arsenic with respect to laterite and sandstone [23]. However, the positive  
181 value for shale ( $0.011 \text{ kJ/mol}$ ) indicates an increase in randomness at the interface between the solid and the solution during  
182 the sorption process [8]. The isotherm being carried out at a concentration close to equilibrium could justify this result of  
183 positive  $\Delta S$  for shale. Because Coulibaly [24] obtained during his work with shale a negative  $\Delta S$  value before reaching  
184 equilibrium and a positive value close to equilibrium. The author therefore deduced from this that two different processes  
185 can govern the adsorption process for the same material. The  $\Delta G^\circ$  values are negative at certain temperatures for laterite  
186 and sandstone, confirming the spontaneity of the sorption process. In contrast, the  $\Delta G^\circ$  values for shale are positive across  
187 various temperatures. But, the decrease in the value of  $\Delta G^\circ$  from  $4.59$  to  $4.35$  with a change in temperature from  $20$  to  $40$   
188 °C suggests that a higher temperature is favorable for adsorption. Thus, if the temperature is high enough, the reaction will  
189 occur spontaneously [8]. In addition to physisorption, other mechanisms such as ligand exchange and electrostatic  
190 interactions may also be involved [6].





B



C

**Fig. 3.** Variation of the adsorption constant as a function of temperatures (20, 30, 40°C) on laterite (A), sandstone (B), and shale (C).

**Table I:** Thermodynamic data for arsenic adsorption on laterite, sandstone, and shale

	Temperature (°C)	$\Delta G$ (kJ/mol)	$\Delta H$ (kJ/mol)	$\Delta S$ (kJ/ mol <sup>-1</sup> )
Laterite	20	-2.87	55.94	-0.180
	30	0.38		
	40	0.71		
sandstone	20	1	45.357	-0.154
	30	-3.258		
	40	-1.962		
shale	20	4.59	-8.083	0.011
	30	4.541		
	40	4.35		

### 3.3 Isotherm Modeling

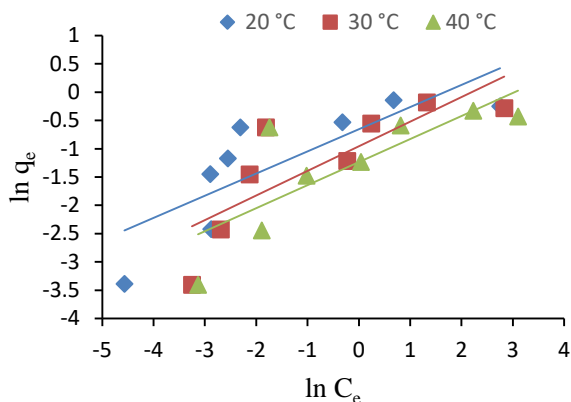
The Freundlich, Langmuir, Elovich, Dubinin–Radushkevich, and Temkin models were used to describe the adsorption isotherms.

#### 3.3.1 Freundlich Model

Fig. 4 presents the Freundlich isotherm corresponding to the arsenic adsorption data on the materials. The Freundlich parameters ( $K_f$  and  $n_f$ ) and the correlation coefficient are summarized in Table II. For all adsorbents and temperature ranges considered, the correlation coefficients ( $R^2$ ) range from 0.790 to 0.979. Therefore, the experimental data can be fitted to the

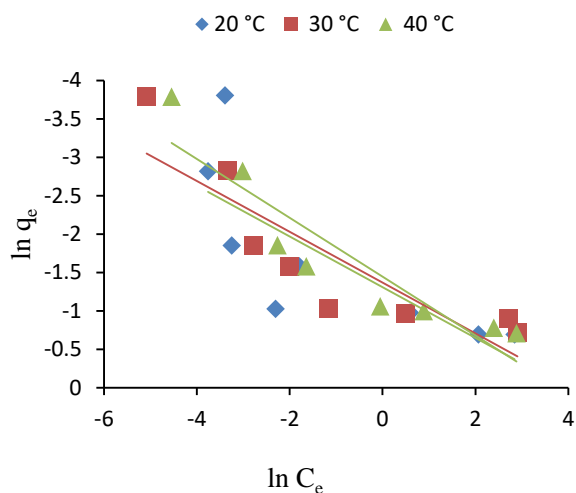
219 Freundlich model. For all three materials, the values of  $n$  were between 1 and 4, indicating favorable adsorption [25]. The  
220 results suggest easy separation and favorable adsorption of arsenic ions on the heterogeneous surface of the adsorbents.  
221 By comparing the  $K_f$  values for laterite (0.320 to 0.519), sandstone (0.235 to 0.269), and shale (0.049 to 0.057), the  
222 adsorption capacity of arsenite ions on these geomaterials follows the order: laterite > sandstone > shale. The Freundlich  
223 exponent  $1/n$  values were all below unity, indicating the microporous nature of the materials according to Giles et al. [13],  
224 and a reduction in available adsorption sites as solution concentration increases. The  $R^2$  values are lower than those of  
225 Tiendrébéogo et al. [26] which is 0.99. For these authors the Freundlich isotherm model was the best-fit model of the  
226 experimental data during their study arsenic adsorption on modified laterites. Therefore, As(III) removal could occur by  
227 multilayer adsorption.

228  
229  
230



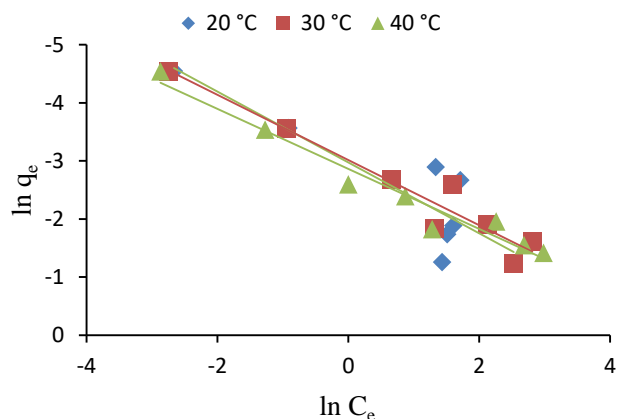
A

231



B

232



C

233  
234  
235

**Fig. 4.** Linear representation at different temperatures (20, 30, 40°C) according to the Freundlich model for arsenic adsorption on laterite (A), sandstone (B), and shale (C).

236  
237  
238

Table II: Parameters related to the Freundlich model

Temperatures	Constants	Materials		
		laterite	sandstone	shale
20°C	$n_f$	2.203	3.028	1.639
	$K_F$ (mg/g)	0.320	0.269	0.051
	$R^2$	0.809	0.923	0.893
30°C	$n_f$	2.609	3.023	1.78
	$K_F$ (mg/g)	0.341	0.254	0.049
	$R^2$	0.790	0.875	0.964
40°C	$n_f$	2.553	2.612	1.937
	$K_F$ (mg/g)	0.519	0.235	0.057
	$R^2$	0.809	0.923	0.979

239

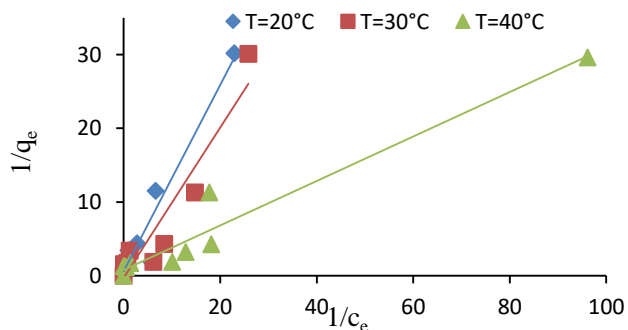
240 **3.3.2 Langmuir Model**

241 The application of the Langmuir model to the experimental data from arsenic adsorption by laterite, sandstone, and shale  
 242 is presented in Fig. 5. The parameters related to the model are summarized in Table III. The high values of the correlation  
 243 coefficient ( $R^2 > 0.95$ ) indicate a good fit of the model. The Langmuir isotherm accurately describes the adsorption of arsenite  
 244 ions on all three materials. The separation or equilibrium factor ( $R_L$ ), ranging between 0 and 1, indicates that the isotherm  
 245 is favorable [27]. As the initial concentration increases, the isotherm becomes more favorable and irreversible, the values  
 246 of the separation factor approach zero. The Langmuir model provided the best fit for arsenic adsorption on all three supports.  
 247 This supports the idea that adsorption occurs on a homogeneous monolayer surface without interaction between adsorbed  
 248 molecules according Khanzada et al. [6]. However, the adsorption capacity is almost of the same order (0.2 - 0.827 mg/g)  
 249 as that obtained by Gimenez et al. [28] during the adsorption of arsenic on hematite, magnetite and natural goethite.

250 **Table III:** Parameters related to the Langmuir model.

Temperatures	Constants	Materials		
		laterite	sandstone	shale
20 °C	$q_{mL}$ (mg/g)	1.627	0.539	0.135
	$R^2$	0.968	0.945	0.975
	$K_L$ (L/mg)	0.486	3.164	1.473
	$R_L$	0.291	0.059	0.119
30 °C	$q_{mL}$ (mg/g)	0.645	0.309	0.114
	$R^2$	0.947	0.984	0.981
	$K_L$ (L/mg)	0.316	12.389	1.562
	$R_L$	0.387	0.015	0.113
40 °C	$q_{mL}$ (mg/g)	1.276	0.340	0.135
	$R^2$	0.973	0.991	0.990
	$K_L$ (L/mg)	2.598	6.534	1.473
	$R_L$	0.071	0.029	0.119

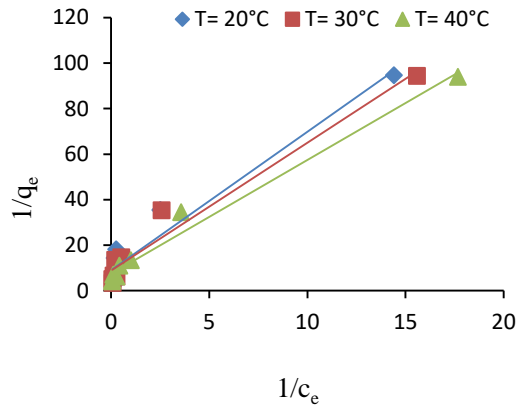
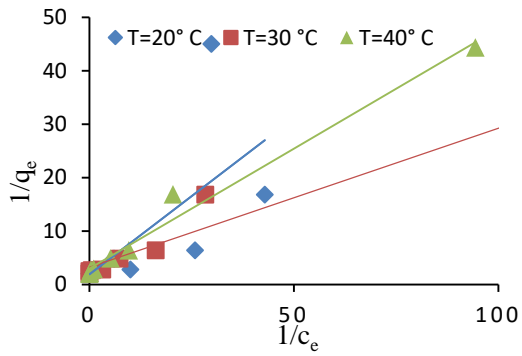
251  
252  
253  
254



A

255

B

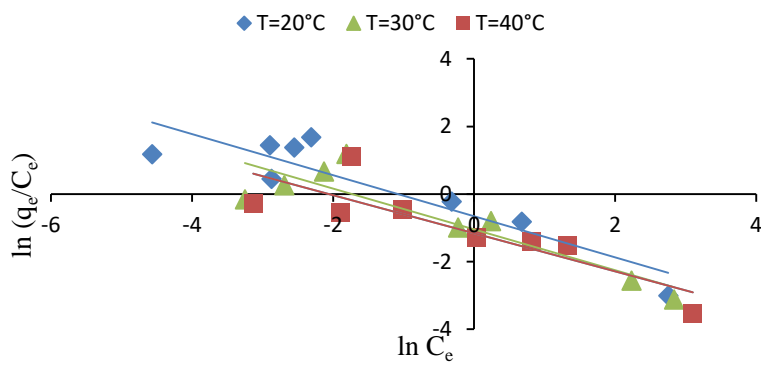


C

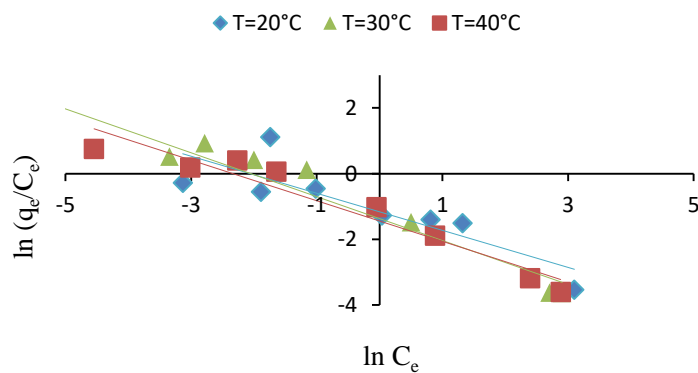
**Fig. 5.** Representation according to the Langmuir model for arsenic adsorption at different temperatures (20, 30, and 40 °C) on laterite (A), sandstone (B), and shale (C).

### 3.3.3 Elovich Model

The linearization plot based on the Elovich equation is highlighted in Fig. 6. Table IV presents the model constants and the corresponding  $R^2$  values. The  $R^2$  values range from 0.787 to 0.819 for laterite, 0.582 to 0.932 for sandstone, and 0.473 to 0.883 for shale. Given these  $R^2$  values, the adsorption data did not fit the model well. Therefore, within the studied concentration range, it is unlikely that multilayer adsorption occurs for arsenic adsorption on laterite, sandstone, and shale.



A



B

C

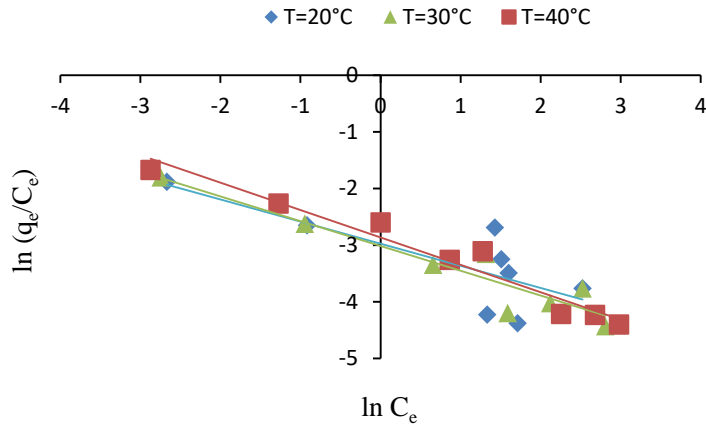


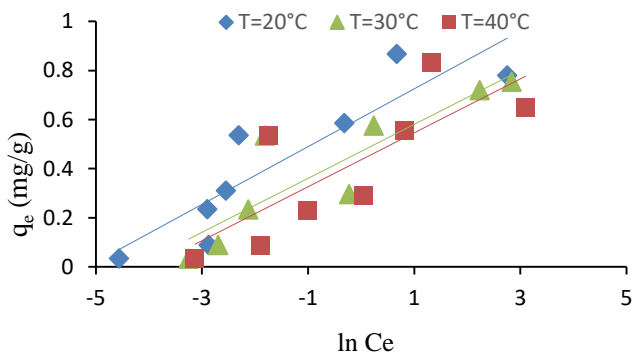
Fig. 6. Linear representation based on the Elovich equation for arsenic adsorption at different temperatures (20, 30, and 40 °C) on laterite (A), sandstone (B), and shale (C).

Table IV: Parameters related to the constants of the Elovich equation.

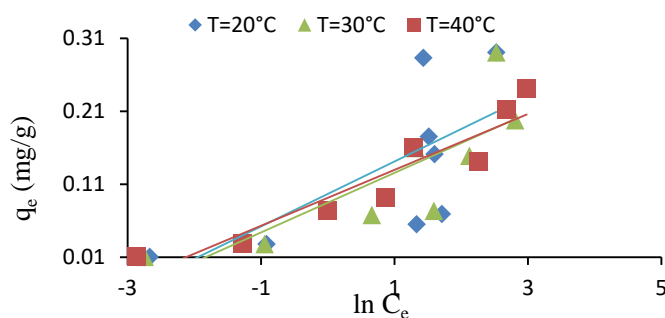
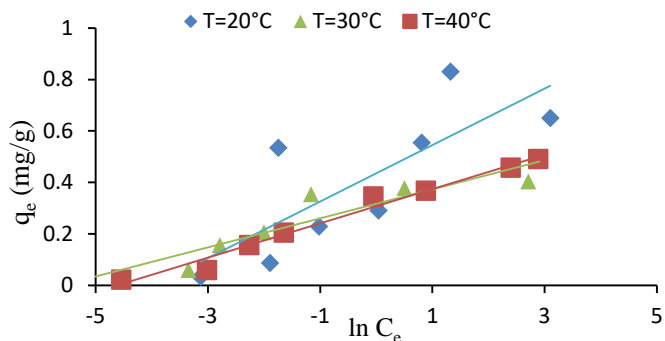
Temperatures	Constants	Materials		
		laterite	sandstone	shale
20 °C	$q_{mE}$ (mg/g)	2.258	3.414	5.053
	$R^2$	0.787	0.581	0.473
	$K_E$ (L/mg)	0.084	0.089	0.008
30 °C	$q_{mE}$ (mg/g)	1.906	1.423	2.615
	$R^2$	0.819	0.932	0.883
	$K_E$ (L/mg)	0.119	0.223	0,016
40 °C	$q_{mE}$ (mg/g)	1.643	1.620	2.067
	$R^2$	0.907	0.968	0.976
	$K_E$ (L/mg)	0.316	0.145	0.027

### 3.3.4 Temkin Model

The constants obtained from the linear form of the Temkin model (Fig. 7) are presented in Table V. According to the table, the Temkin model does not fit the experimental results well, as the correlation coefficients are low. For laterite, the adsorption energy variation ( $\Delta b_T$ ) decreases with increasing temperature, with values of 23.988, 23.577, and 22.101 kJ/mol at 20, 30, and 40 °C, respectively. In contrast, for sandstone and shale,  $\Delta b_T$  shows no clear trend with temperature increase. It ranges from 23.480 to 39.092 kJ/mol for sandstone and from 58.307 to 67.977 kJ/mol for shale. These variations in adsorption energy derived from the Temkin model confirm the findings from the temperature effect analysis for sandstone and shale. Overall, the high binding energy values ( $b_T$  greater than 8 kJ/mol which refers to physisorption thresholds) suggest that chemisorption may contribute to arsenic adsorption to some extent on laterite, sandstone, and shale [29]. The adsorption energy variations from the Temkin model confirm the temperature effect analysis. According to Al-Ghouthi and Da'ana [30] this isotherm model is not appropriate to present complex adsorption systems including aqueous phase adsorption isotherms.



A



C

**Fig. 7.** Linear representation according to the Temkin model for arsenic adsorption at different temperatures (20, 30, and 40 °C) on laterite (A), sandstone (B), and shale (C).

**Table V:** Parameters related to the Temkin model.

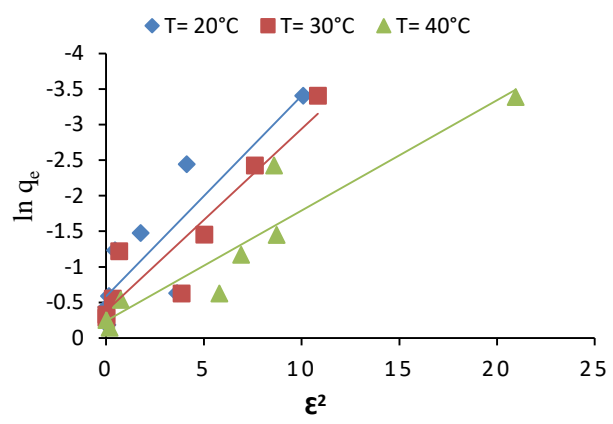
Temperatures	Constantes	Materials		
		laterite	sandstone	shale
20 °C	$b_T$ (KJ/mol)	23.988	23.480	58.307
	$K_T$ (L/mg)	1.015	1.014	1.026
	$R^2$	0.847	0.966	0.897
30 °C	$b_T$ (KJ/mol)	23.577	39.816	51.436
	$K_T$ (L/mg)	1.014	1.020	1.022
	$R^2$	0.906	0.978	0.901
40 °C	$b_T$ (KJ/mol)	22.101	39.092	67.977
	$K_T$ (L/mg)	0.813	1.019	2.349
	$R^2$	0.898	0.989	0.938

### 3.3.5 Dubinin–Radushkevich (D-R) Model

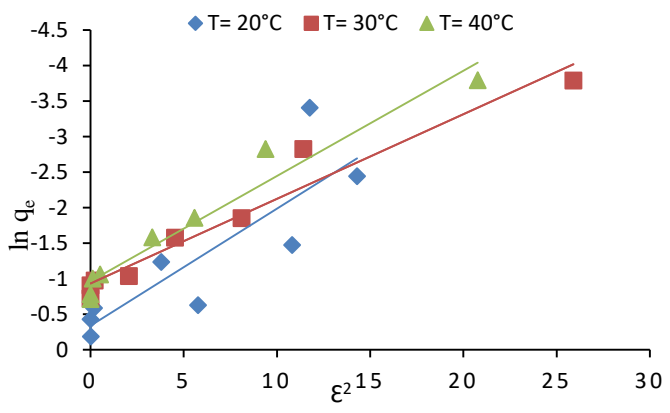
Fig. 8 presents the D-R model, and the corresponding parameters are shown in Table VI. The maximum adsorption capacity ( $q_{max}$  D-R) increases with rising temperature for laterite. In contrast, for sandstone and shale, the model generally indicates a decrease in  $q_{max}$  D-R as temperature increases. The correlation coefficients at 30 and 40 °C range from 0.8 to 0.976, which are close to 1 for all three materials (laterite, sandstone, and shale). This suggests that the D-R isotherm model is not applicable across all temperature ranges. According to the model, only the isotherms at 30 and 40 °C for arsenic retention on laterite, sandstone, and shale are favorable. Additionally, at these temperatures, the mean adsorption energies are laterite 1.397 and 1.795 kJ/mol, sandstone 2.049 and 1.837 kJ/mol and shale 1.216 and 1.244 kJ/mol. The mean adsorption energy values ( $E$ ) are all below the threshold of 8 kJ/mol, indicating that physisorption is likely the dominant process at these temperatures [31] [10].

In contrast, Al-Ghouthi and Sweleh [32], in their study on the removal by adsorption of mercury from water by adsorbents derived from date kernels, distinguished the physical and chemical adsorption of  $Hg^{2+}$  ions by calculating the average free energy.

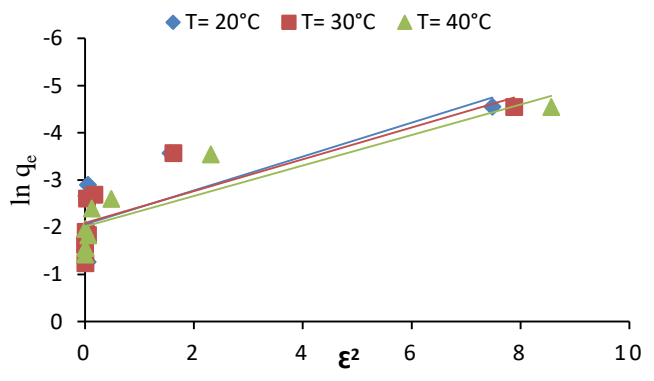
312  
313  
314  
315  
316  
317  
318  
319  
320  
321



A



B



C

322

323  
324  
325  
326  
327  
328  
329

Fig. 8. Linear representation according to the Dubinin–Radushkevich (D-R) model for arsenic adsorption at different temperatures (20, 30, 40°C) on laterite (A), sandstone (B), and shale (C).

Table VI: Parameters related to the Dubinin–Radushkevich model.

Temperatures	Constants	Materials		
		laterite	sandstone	shale
20 °C	$q_m$ D-R (mg/g)	0.556	0.713	0.127
	$\beta$ (mol <sup>2</sup> /KJ <sup>-2</sup> )	0.282	0.165	0.359
	E (KJ/mol)	1.332	1.742	1.179
	R <sup>2</sup>	0.873	0.855	0.80
30 °C	$q_m$ D-R (mg/g)	0.684	0.393	0.124
	$\beta$ (mol <sup>2</sup> /KJ <sup>-2</sup> )	0.256	0.119	0.338
	E (KJ/mol)	1.397	2.049	1.216
	R <sup>2</sup>	0.932	0.975	0.84

40 °C	$q_m$ D-R (mg/g)	0.785	0.380	0.133
	$\beta$ (mol <sup>2</sup> /KJ <sup>-2</sup> )	0.155	0.148	0.323
	E (KJ/mol)	1.795	1.837	1.244
	R <sup>2</sup>	0.939	0.976	0.897

## 4. CONCLUSION

These isotherms are classified as type L, which typically indicates microporous adsorbents with strong adsorbate adsorbent affinity. The negative values of  $\Delta G^\circ$  obtained with certain temperature on laterite (-2.87 kJ/mol) and sandstone (-1.962 - 3.258 kJ/mol) indicated that the arsenic adsorption is spontaneous process. The negative values of  $\Delta H^\circ$  (-8.083 kJ/mol) on the shale represent an exothermic process and suggest a physisorption behavior. The negative values of  $\Delta S^\circ$  with the laterite (-0.180 kJ/mol) and sandstone (-0.154 kJ/mol) suggest that a significant change does not happen in the internal structure of adsorbent during the adsorption of As. The adsorption isotherm studies of arsenic on laterite, sandstone, and shale indicate that the Langmuir model best describes the adsorption process. The Temkin isotherm suggests that chemisorption may contribute to arsenic adsorption to some extent on all three materials. The mean adsorption energy derived from the Dubinin–Radushkevich model identifies physisorption as a key mechanism in arsenic adsorption. Overall, laterite, sandstone, and shale are low-cost adsorbents that can be effectively used for arsenic removal from water. Field application studies or pilot scale trials could be conducted for future studies.

## COMPETING INTERESTS

Authors have declared that no competing interests exist.

## AUTHORS' CONTRIBUTIONS

This work was carried out in collaboration among all authors. All authors read and approved the final.

## REFERENCES

- Bhardwaj, A., Rajput, R.; Misra, K. Chapter 9—Status of Arsenic Remediation in India. In *Advances in Water Purification Techniques*; Ahuja, S., Ed.; Elsevier: Amsterdam, The Netherlands, 2019; 219–258. ISBN 978-0-12-814790-0.
- Algieri, C.; Pugliese, V.; Coppola, G.; Curcio, S.; Calabro, V.; Chakraborty, S. Arsenic Removal from Groundwater by Membrane Technology: Advantages, Disadvantages, and Effect on Human Health. *Groundw. Sustain. Dev.* 2022, 19, 100815.
- Khatun, J.; Intekhab, A.; Dhak, D. Effect of Uncontrolled Fertilization and Heavy Metal Toxicity Associated with Arsenic(As), Lead(Pb) and Cadmium (Cd), and Possible Remediation. *Toxicology* 2022, 477, 153274.
- Zhiliang, L., Guining, L., Daolin, D., Dongye, Z., Harnessing low-cost adsorbents for removal of heavy metals and metalloids in contaminated water: Progress in the past decade and future perspectives *Journal of Cleaner Production*, 2025; 518, 145845
- Xu, Z., Cai, J.-g., Pan, B.-c., Mathematically modeling fixed-bed adsorption in aqueous systems. *J. Zhejiang Univ. Sci. A*, 2013;14 (3), 155–176. <https://doi.org/10.1631/jzus.A1300029>.
- Khanzada, A.K.; Rizwan,M.; Al-Hazmi, H.E.; Majtacz, J.;Kurniawan, T.A.; M ,akinia, J. Removal of Arsenic from Wastewater Using Hydrochar Prepared from Red Macroalgae: Investigating its Adsorption Efficiency and Mechanism. *Water*, 2023 ; 15, 3866. <https://doi.org/10.3390/w15213866>
- Wang J., Guo X. Adsorption isotherm models: Classification, physical meaning, application and solving method. *Chemosphere*, 2020 ; 258, doi.org/10.1016/j.chemosphere.2020.127279.
- Coulibaly S. L., Yvon J. & Coulibaly L. Physicochemical Characterization of Lomo Nord black shale and application as low cost material for phosphate adsorption in aqueous solution. *J. Environ. Earth Sci.* 2015 ; 5 : 42-60.
- Coulibaly, S. L., Akpo, K. S., Yvon, J. & Coulibaly, L. Fourier Transform Infra-Red (FTIR) spectroscopy investigation, dose effect, kinetics and adsorption capacity of phosphate from aqueous solution onto laterite and sandstone. *J. Environ. Manage.* 2016 ; 183 : 1032-1040.
- Zhou, X., Yu, X., Maimaitiniyazi, R., Zhang, X., Qu, Q. Discussion on the thermodynamic calculation and adsorption spontaneity re Ofudje et al. (2023). (2024) 10(8), e28188
- Alsawat, M. Congo red dye adsorption using CuSnO<sub>2</sub>TiO<sub>2</sub> nanocomposites: Adsorption data interpretation by statistical modelling. *International Journal of Electrochemical Science*, 2024, 19, 100611. <https://doi.org/10.1016/j.ijoes.2024.100611>
- Koua-Koffi N. A. A., Coulibaly L. S., Sangare D. & Coulibaly L. (2018). Laterite, sandstone and shale as adsorbents for the removal of arsenic from water. *Am. J. Analyt. Chem.*, 2018 ; 9: 340-352.

- 382 13. Giles, C. H., Evans, M. M. C., Nakhawas, S. W. & Smith, D. J. Studies in adsorption. Part XI. A system of classification  
383 of solution adsorption isotherms, and its use in diagnosis of adsorption mechanisms and in measurement of specific  
384 surface areas of solids. *J. Chem. Soc.*, 1960; 3973-3993.
- 385
- 386 14. Kabdasli, I., Gurel, M. & Tunay, O. Characterisation and treatment of textile printing waste waters. *Environ. Technol.*  
387 2000 ; 21 : 1147-1155
- 388
- 389 15. Feng-Chin, W., Ru-Ling, T. & Ruey-Shin, J. Characteristics of Elovich equation used for the analysis of adsorption  
390 kinetics in dye-chitosan systems. *Chem. Eng. J.*, 2009 ; 150 : 366-373.
- 391 16. Kim, Y., Kim, C., Choi, I., Rengraj, S. & Yi, J. Arsenic removal using mesoporous alumina prepared via a templating  
392 method. *Environ. Sci. Technol.* 2004 ;38 : 924-931.
- 393 17. Belaid, K. D., Kacha, S. Étude cinétique et thermodynamique de l'adsorption d'un colorant basique sur la sciure de bois.  
394 *J. Water Sci.* 2010 ; 24(2) : 131-144.
- 395 18. Mondal, P., Balomajumder, C. & Mohanty, B. A laboratory study for the treatment of arsenic, iron, and manganese  
396 bearing ground water using Fe<sup>3+</sup> impregnated activated carbon : effects of shaking time, pH and temperature. *J. Hazard.*  
397 *Mater.*, 2007; 144 : 420-426.
- 398 19. Ziati, M., Hazourli, S., Nouacer, S. & Khelaifia, F. Z. Elimination of arsenic (III) by adsorption on coal resulting from date  
399 pits and activated thermally and chemically. *Water Qual. Res. J.*, 2012 ; 47(1) : 91-102.
- 400 20. Parga, J. R., Vazquez, V., and Moreno H. Thermodynamic Studies of the Arsenic Adsorption on Iron Species Generated  
401 by Electrocoagulation. *Journal of Metallurgy*, 2009; 9 p. doi:10.1155/2009/286971
- 402 21. Unuabonah, R. I., Adebowale, K. O. & Owolabi, B. I. Kinetic and thermodynamic studies of the adsorption of lead (II)  
403 ions onto phosphate-modified kaolinite clay. *J. Hazard. Mater.*, 2007 ;144 : 386-395.
- 404 22. Boparai, H. K., Joseph, M. & O'Carroll, D. M. Kinetics and thermodynamics of cadmium ion removal by adsorption onto  
405 nanozerovalent iron particles. *J. Hazard. Mater.*, 2011 ; 186 : 458-465.
- 406 23. Maji, S. K., Pal, A., Pal, T. & Adak, A. Modeling and fixed bed column adsorption of As (III) on laterite soil. *Sep. Purif.*  
407 *Technol.*, 2007 ; 56 : 284-290.
- 408
- 409 24. COULIBALY, S.L. Reduction of phosphates from wastewater by adsorption on geomaterials made of laterite,  
410 sandstone and shale. 2024
- 411
- 412 25. Mahmoud, M.E.; Saad, E.A.; Soliman, M.A.; Abdelwahab, M.S. Synthesis and Surface Protection of Nano Zero valent  
413 Iron (NZVI) with 3-Aminopropyltrimethoxysilane for Water Remediation of Cobalt and Zinc and Their Radioactive Isotopes.  
414 *RSC Adv.*, 2016 ; 6, 66242–66251
- 415
- 416 26. Tiendrébéogo, R., Sanou, Y., Kaboré, R., Paré, S., and Senou, A. Preparation and Characterization of Two Modified  
417 Laterite Soils for Arsenic Removal in Aqueous Solutions: Efficiency and Kinetic Modelling. *International Research Journal*  
418 *of Pure and Applied Chemistry*, 2024 ; 25 (5):1-16. <https://doi.org/10.9734/irjpac/2024/v25i5871>.
- 419
- 420 27. Chaudhry, S. A., Zaidi, Z., Siddiqui, S. I. Isotherm, kinetic and thermodynamics of arsenic adsorption onto Iron-Zirconium  
421 Binary Oxide-Coated Sand (IZBOCS): Modelling and process optimization. *Journal of Molecular Liquids*, 2017; 229, 230-  
422 240 . <https://doi.org/10.1016/j.molliq.2016.12.048>
- 423
- 424 28. Gimenez, J., Martinez, M., Pablo, J., Rovira, M., and Duro, L. Arsenic sorption onto natural hematite, magnetite and  
425 goethite. *Journal of Hazardous Materials*, 2007, 141,575 – 580.
- 426 29. Nemade, P. D., Kadam, A. M. & Shankar, H. S. Adsorption of arsenic from aqueous solution on naturally available red  
427 soil. *J. Environ. Biol.* 2009 ; 30(4) : 499-504.
- 428 30. Al-Ghouti, M. A, Da'ana, D. A. Guidelines for the use and interpretation of adsorption isotherm models: A review. *Journal*  
429 *of Hazardous Materials*, 2020, 393, 122383. <https://doi.org/10.1016/j.jhazmat.2020.122383>.
- 430 31. Ozcan, A. S., Erdem, B. & Ozcan, A. Adsorption of Acid Blue 193 from aqueous solutions onto BTMA-bentonite. *Colloids*  
431 *and Surfaces A: Physicochem. Eng. Aspects*, 2005 ; 266 : 73-81.
- 432 32. Al-Ghouti, M., Sweleh, A., Optimizing textile dye removal by activated carbon prepared from olive stones. *Environ.*  
433 *Technol. Innov.*, 2019,16, 100488.
- 434
- 435
- 436
- 437
- 438
- 439